

# Fabrication of Nonbiofouling Surface and Its Application to Surface Plasmon Field-Enhanced Fluorescence Spectroscopy

Eunkyung Kim<sup>1</sup>, Bong Soo Lee<sup>2</sup>,  
Hyeon-Bong Pyo<sup>3</sup>, Hyun-Woo Song<sup>3</sup>,  
Young-Pil Kim<sup>1</sup>, Insung S. Choi<sup>2</sup> &  
Hak-Sung Kim<sup>1</sup>

<sup>1</sup>Department of Biological Sciences, Korea Advanced Institute of Science and Technology (KAIST), Daejeon 305-701, Korea

<sup>2</sup>Department of Chemistry and School of Molecular Science (BK21), Center for Molecular Design and Synthesis, Korea Advanced Institute of Science and Technology (KAIST), Daejeon 305-701, Korea

<sup>3</sup>BIOMEMS Team, IT Convergence and Components Laboratory, Electronics and Telecommunications Research Institute, Daejeon 305-700, Korea

Correspondence and requests for materials should be addressed to H.-S. Kim (hskim76@kaist.ac.kr)

Accepted 4 April 2008

## Abstract

Reducing the non-specific binding of proteins on a chip surface is essential for the development of biosensors with high sensitivity and specificity. We fabricated poly(oligo(ethylene glycol) methacrylate) (pOEGMA) films with various thicknesses as a non-biofouling surface for surface plasmon field-enhanced fluorescence spectroscopy (SPFS). To accomplish a sensitive SPFS signal, the thickness of the pOEGMA films was controlled by surface-initiated atom transfer radical polymerization (SI-ATRP) on gold-coated glass (Au/Glass) and gold-coated Si (Au/Si) substrates. When fluorophores immobilized on the pOEGMA films were directly excited without a plasmon effect, the fluorescence intensity displayed a linear dependency on the tested thickness of the pOEGMA films on both Au/Si (9-60 nm) and Au/Glass (8-56 nm). As a result, the surface plasmon field-induced fluorescence intensity on Au/Glass enabled thickness-dependent sensitivity. The SPFS signal on 50-nm-thick pOEGMA films was estimated to be 100-fold stronger than that on 13-nm-thick pOEGMA films. Since the SPFS on pOEGMA film can allow an easy conjugation of biomolecules and provide a high resistance to biofouling events, our fabricated system has a great potential as a platform for biosensors with high sensitivity.

**Keywords:** Nonbiofouling surface, Poly(oligo(ethylene

glycol) methacrylate) films, Surface plasmon field-enhanced fluorescence spectroscopy, Biosensor

## Introduction

The development of biosensors with high sensitivity and specificity has been of great significance in many areas. Many methods have been devised to construct biosensors with a desired performance. Among these methods, surface plasmon resonance (SPR) spectroscopy has been widely used because it enables the sensitive detection ( $\text{ng}/\text{cm}^2$ ) of biomolecules in a label-free and real-time manner<sup>1-3</sup>. Despite the powerful use of SPR biosensors, several formidable limitations still remain. One of the major problems is the detection sensitivity of low-mass molecules. Since SPR is based on a change in the refractive indexes of analytes, substances with low molecular weight or substances occurring at low concentrations often cause subtle changes in the refractive index, thus resulting in a poor detection limit<sup>2</sup>.

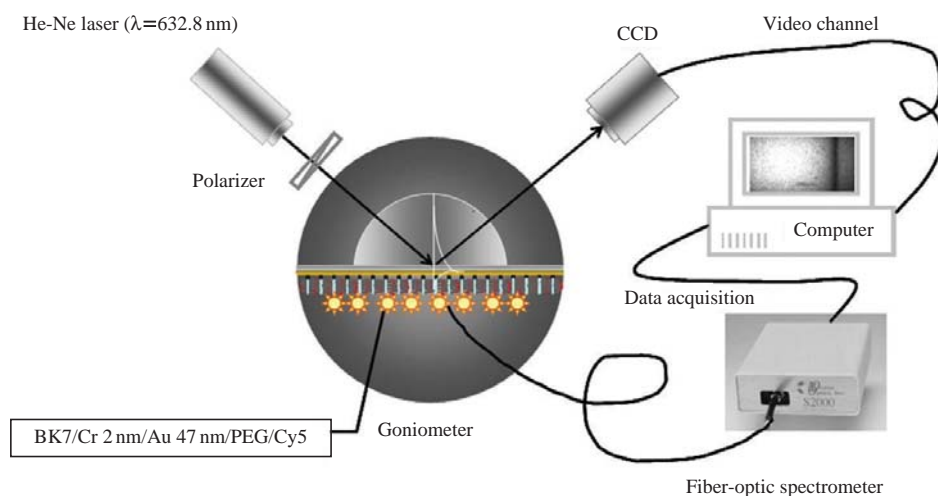
As a consequence, surface plasmon field-enhanced fluorescence spectroscopy (SPFS), which combines surface plasmon resonance (SPR) with fluorescence spectroscopy, was developed. Since its introduction in 2000<sup>4</sup>, it has been applied to characterize the interactions of oligonucleotides<sup>5</sup> and proteins<sup>6</sup>, and has showed good performance in terms of sensitivity and reliability. In principle, SPFS allows the use of fluorophores within an evanescent field induced by surface plasmon on a metal surface<sup>4</sup>. In addition to the increased refractive index of molecules, the subsequent excitation of fluorophores at an interface between metal and a dielectric medium is necessarily accompanied with a more enhanced signal generation than in SPR only. Therefore, the detection limit for low-mass compounds, which cause small changes in refractive index, can be improved in the presence of fluorophores. However, since fluorescence is governed by the SPR-induced evanescent field, which typically exhibits an exponential decay based on distance, the intensity is indeed dependent on the distance between the fluorophore and metal surface. Although only fluorophores within the evanescent field can be excited, they can reduce the fluorescent signal in close proximity of the metal surface because the metal acts as a very efficient quencher that absorbs

all the excitation energy of the fluorophores<sup>7</sup>. Thus, the fluorophores should be located within the range of the evanescent field and be separated enough to avoid quenching by the metal. In an effort to overcome this drawback, a metal surface was coated using various methods including a layer-by-layer strategy<sup>8</sup>, carboxymethyl dextran (CMD)<sup>9</sup>, and a plasma-polymerized allylamine (ppAA)<sup>5</sup>. However, these approa-

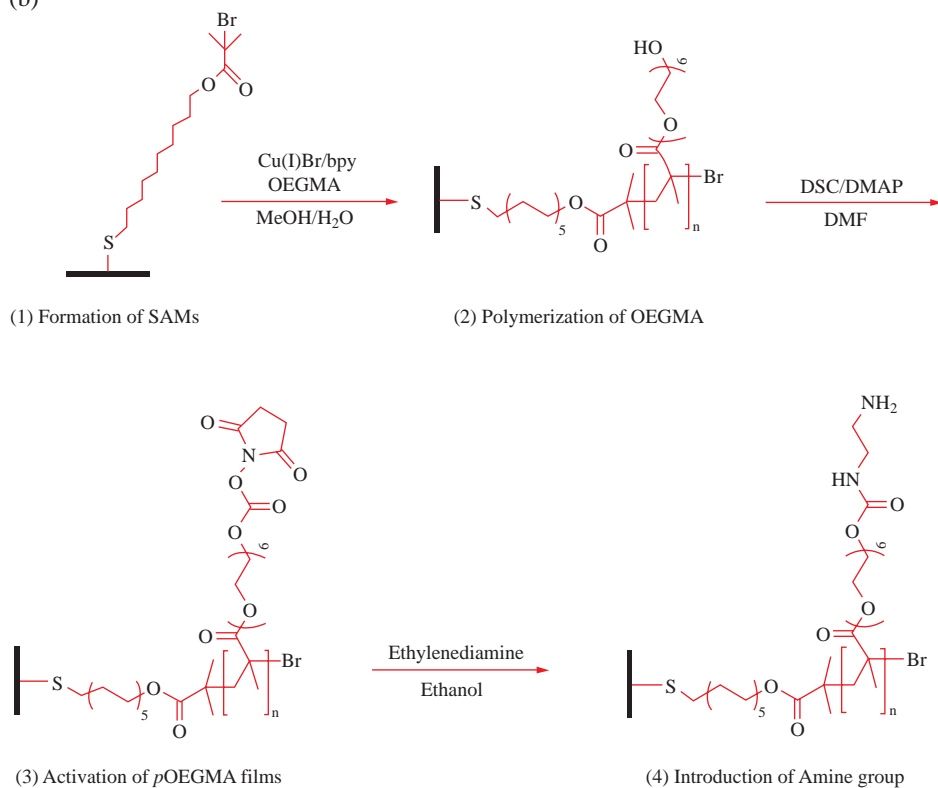
ches have some limitations with respect to the reduction in non-specific protein binding and the precise distribution of biomolecules.

In the present study, we report on the fabrication of nonbiofouling poly(oligo(ethylene glycol) methacrylate) (*p*OEGMA) films and its application to SPFS. The ability of surface coatings containing poly(ethylene glycol) (PEG) to prevent non-specific protein ad-

(a)



(b)



**Scheme 1.** (a) Schematic illustration of the SPFS system. A TM-polarized He-Ne laser was used as a pumping source of Cy5 dye, as well as for the surface plasmon excitation of the gold layer. The SPR angle was monitored using a CCD camera, and the enhanced Cy5 fluorescence was observed spectrally using a fiber-optic spectrometer. (b) Schematic representation of SI-ATRP procedures of *p*OEGMA film.

**Table 1.** Thickness changes after SAM formation and polymerization on Au/Si and Au/Glass substrates, and water static contact angles according to the thickness of the *p*OEGMA films.

No.	After SAMs formation		After polymerization				
	Thickness (nm)		Thickness (nm)			Contact angle (°)	
	Au/Si	Au/Glass	Au/Si	Au/Glass <sup>a</sup>	Au/Glass <sup>b</sup>	Au/Si	Au/Glass
1	1.1 ± 0.1	1.2 ± 0.8	9.1 ± 0.6	7.5 ± 0.3	11.1	44.1	43.6
2	1.2 ± 0.0	0.8 ± 0.8	21.8 ± 0.3	20.2 ± 0.6	19.9	45.0	46.1
3	1.3 ± 0.1	0.6 ± 0.1	42.2 ± 1.6	37.1 ± 0.9	35.3	47.6	52.4
4	1.3 ± 0.1	1.3 ± 0.6	59.5 ± 2.6	55.8 ± 8.0	47.1	49.0	52.4

<sup>a</sup>All of the thicknesses except for b were measured by ellipsometry. <sup>b</sup>The thicknesses were estimated from SPR spectra.

sorption has been intensively investigated over the past decades<sup>10-13</sup>. Although PEG is effective in preventing nonspecific protein adsorption, its nonfouling ability depends on the surface chain density. PEG-based, nonbiofouling surfaces were constructed using surface-initiated atom transfer radical polymerization (SI-ATRP) on a gold-coated glass substrate (Au/glass). The resulting surfaces with various thicknesses were investigated in terms of the enhancement of fluorescence intensity, the details of which are reported herein.

## Results and Discussion

For the measurements of SPFS (Scheme 1a), a Au/Glass substrate was used. Recently, it was reported that intact *p*OEGMA films were grown from gold-coated Si (Au/Si) chips with different thicknesses, and that the hydroxyl group of OEG was activated with *N,N'*-disuccinimidyl carbonate (DSC)<sup>14</sup>. In addition, an amide coupling reaction was utilized for the immobilization of biomolecules.

As illustrated in Scheme 1b, the self-assembled monolayers (SAMs) of ATRP initiator-containing disulfide, [BrC(CH<sub>3</sub>)<sub>2</sub>COO-(CH<sub>2</sub>)<sub>11</sub>S]<sub>2</sub>, were formed by immersing each substrate in a 1mM ethanolic solution of the disulfide for 12 h at room temperature. The resulting SAMs were characterized using contact angle goniometry and ellipsometry. The ellipsometric thickness of the SAMs on Au/Glass was estimated to be 9.80 ± 5.56 Å on average, which indicates a relatively larger deviation than 12.21 ± 0.86 Å of Au/Si due to the roughness of the glass substrate. The water static contact angle was 66.19°, which is almost similar to the water contact angle of 68.04° for Au/Si.

Polymerization was carried out by soaking any substrate of ATRP initiator-presenting SAMs in a water/methanol mixture with oligo(ethylene glycol) methacrylate (OEGMA) and copper(I)bromide/2,2'-dipyridyl in an oxygen-free environment. The polymer brushes

of the *p*OEGMA films were synthesized from pure SAMs on a gold surface as a function of reaction time, and the thickness of the brushes was measured using ellipsometry. The film thicknesses were found to range from 5 to 60 nm (Table 1). The thicknesses of the *p*OEGMA films on Au/Glass were not significantly different from those on Au/Si, but they exhibited a slightly large deviation as can be seen by the SAMs formation. The water contact angle of the polymer surface on Au/Glass was changed from 66.19° to 43.63°, which was similar to the change on Au/Si. This result indicates an increase in hydrophilicity due to the grafted polymers. In addition, the static contact angles also increased up to 52.41° with increasing layer thickness of the *p*OEGMA film due to an increase in the hydrophobicity of the carbon backbone. It is obvious that polymer brushes of tunable thickness within the range of 5 to 60 nm can be easily prepared using a surface-initiated ATRP method. On the other hand, since the ellipsometric thickness on Au/Glass showed a larger deviation than that on Au/Si, we tested the thickness of the *p*OEGMA films on Au/Glass using SPR (Table 1). The thickness of each film was estimated from SPR spectra, and no significant change was observed between the ellipsometry and SPR measurements.

Prior to measuring SPFS, namely investigating the fluorescence intensity with respect to the thickness of *p*OEGMA, we activated the surface with *N*-hydroxysuccinimide (NHS) carbonate ester groups by *N,N'*-disuccinimidyl carbonate (DSC) and 4-(dimethylamino)pyridine (DMAP) in *N,N'*-dimethylformamide (DMF), followed by the introduction of an amine group using ethylenediamine. Then, a pattern generation was achieved using microcontact printing (μCP) of reactive Cy3 dyes containing a bisfunctional NHS ester group with oxidized PDMS stamps that had circle features with a diameter of 30 μm and different spacing onto amine-terminated *p*OEGMA film surfaces. The resulting patterns were examined using fluorescence microscopy (Figure 1). As expected, the

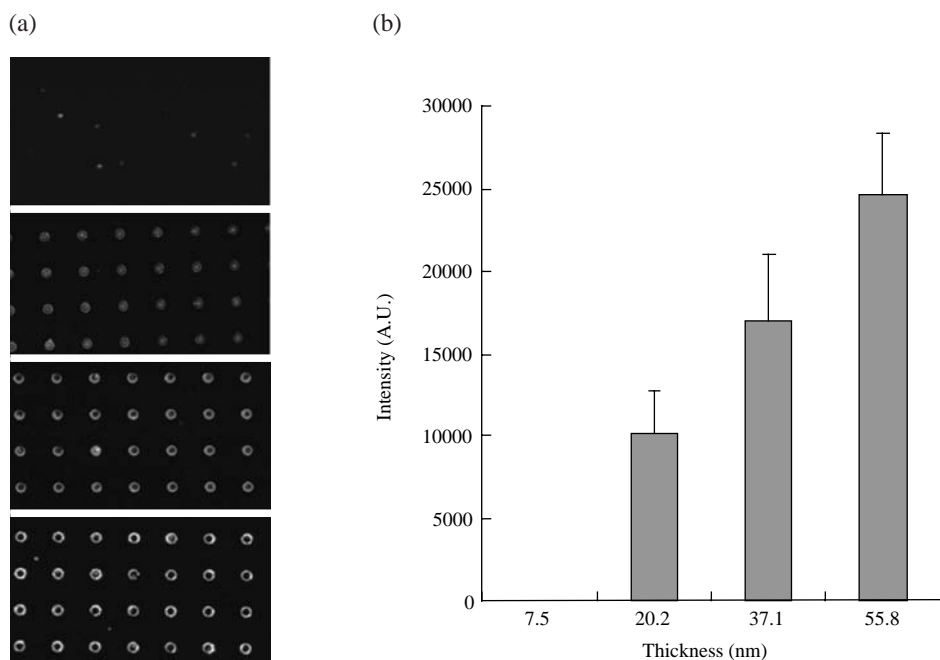


**Figure 1.** Fluorescence intensity with respect to the thickness of *p*OEGMA films on a Au/Glass substrate (a) Fluorescence images by fluorescence spectroscopy. The thickness of the *p*OEGMA films were 7.5, 20.2, 37.1, and 55.8 nm. (b) The fluorescence intensity of Cy3 was analyzed at each thickness of the *p*OEGMA films. The mean value and standard deviation were calculated for 24 spots.

intensity of the fluorescence was quenched by the gold surface with the thickness of the *p*OEGMA film being less than 10 nm. However, as the thickness of *p*OEGMA films increased over 10 nm, the fluorescence intensities also increased, showing a similar result to that on Au/Si (data not shown). The increase of fluorescence intensity seems to be mainly due to the metal-induced effect. Since first reported by Sokolov *et al.*<sup>15</sup>, metal-enhanced fluorescence (MEF) has been studied extensively during the past decade<sup>16-18</sup>. Recently, Zhang and Lakowicz investigated the effects of the thickness of a gold surface on the emission spectra of an AlexaFluor-555 labeled antibody (Alexa-IgG)<sup>19</sup>. They reported that the intensity of the labeled IgG increased with the increasing mass thickness of gold, reaching saturation above 30 nm. The fluorescence intensity increased by 6-fold for an approximate thickness of 30 nm. Therefore, the metal-induced effect seems to make a significant contribution to the increase of fluorescence intensity. Another reason is an increase in the number of amine-functional groups. The thicker the *p*OEGMA films are, the more NHS-activated Cy3 that can be attached to their surfaces.

For the measurements of SPFS, we prepared Cy5-labeled *p*OEGMA films with different thicknesses ranging from 12.8 to 57.3 nm on a Au/Glass substrate. The Cy5 fluorophore (absorption maximum at 649 nm) was excited using a helium-neon laser at a wavelength of 632.8 nm, adjusting the integration time. When a resonantly absorbed plasmon-coupling was monitored by a charge-coupled device (CCD) to find

the minimum level of reflected light, the angles of surface plasmon excitation on the *p*OEGMA films were found to be 43.6° and 58.3°, respectively, for the thicknesses of 12.8 nm and 57.3 nm. These angles were considerably coincident with theoretical angles, 45.3° and 62.5°, respectively. When the Cy5 fluorophore was excited, an emission peak at 683 nm appeared. This indicates a slight shift from 670 nm. On the other hand, the fluorescence intensity induced by surface plasmon excitation on 57.3-nm-thick *p*OEGMA film caused a drastic increase, compared to that on 12.8-nm-thick *p*OEGMA film (Figure 2). The intensity on the 57.3 nm thickness was enhanced about 100-fold over that of the 12.8 nm thickness. This indicates that the fluorescence yield depends strongly on the separation distance from the gold surface, and that there is an optimal distance in SPFS. As has been previously mentioned, when fluorophores are in proximity of a metal surface, the fluorescence signal exhibits a pronounced distance-dependent behavior. Particularly, for a short distance range (<10-15 nm), the fluorescence can be quenched by a reduced lifetime and intensity. For a slightly larger distance range (~20 nm), the red-shifted fluorescence light by optically excited fluorophores can be effectively coupled back to the metal substrate<sup>4</sup>. Beyond this range, as the distance increases, the exponential decay of a surface plasmon field results in a reduction of fluorescence intensity. Due to these effects, there is an optimal distance for SPFS.

Based on these results, we demonstrated that the

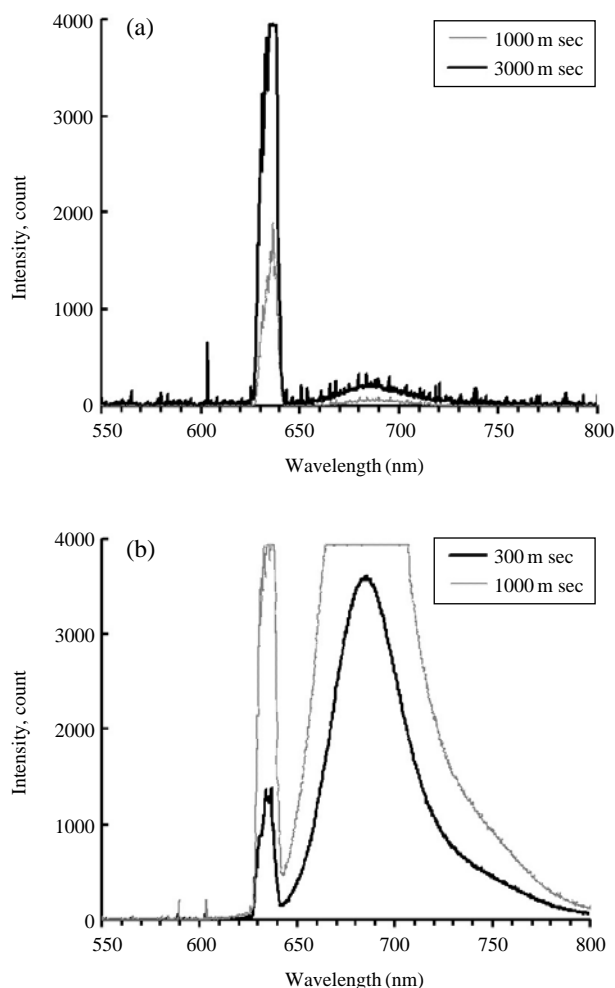


**Figure 2.** SPFS measurements of Cy5 molecules covalently linked to *p*OEGMA films with different thickness on a Au/Glass substrate: (a) 12.8 nm and (b) 57.3 nm.

enhanced optical field of a resonantly excited surface plasmon mode can be used for the (bio)-recognition process of a fluorescently labeled analyte by controlling the spacer distance. The thickness-tunable *p*OEGMA films with nonbiofouling effect can be introduced as a spacer for SPFS measurements. Further effort, such as a detailed study of biomolecular interactions on this nonbiofouling surface, will improve the sensitivity of SPFS as a biosensor.

## Conclusion

In conclusion, we fabricated nonbiofouling *p*OEGMA films with various thicknesses as a spacer model for SPFS, and investigated the effect of *p*OEGMA film thickness on SPFS measurements. Due to the

effects of fluorescence quenching by a metal surface and the decaying efficiency of an SPR evanescent field, there is an optimal spacer thickness for SPFS. Our results showed that the surface plasmon field-induced fluorescence intensity on Au/Glass enabled thickness-dependent sensitivity. The SPF signal on 50-nm-thick *p*OEGMA films was estimated to be 100-fold stronger than that on 13-nm-thick *p*OEGMA films. This indicates that tunable *p*OEGMA films can be effectively applied to SPFS. In addition, *p*OEGMA films have active functional groups for the conjugation of biomolecules and a nonbiofouling property for the prevention of non-specific binding. With these distinct characteristics, the present system has great potential for the development of a biosensor with high sensitivity and specificity.

## Materials and Methods

### Materials

Absolute ethanol (EtOH, 99.9+%, Merck), absolute methanol (MeOH, 99.9+%, Merck), anhydrous *N,N'*-dimethylformamide (DMF, 99.8+%, Aldrich), toluene (J.T. Baker), copper (I) bromide (Cu (I) Br, 99.999%, Aldrich), 2,2'-dipyridyl (bpy, 99+%, Aldrich), *N,N'*-disuccinimidyl carbonate (DSC, Aldrich), and 4-(dimethylamino)pyridine (DMAP, Fluka) were used as received. Poly(ethylene glycol) methacrylate (OEGMA, Mn: ~360, Aldrich) was passed through a column of activated, basic aluminum oxide to remove inhibitors.  $[\text{BrC}(\text{CH}_3)_2\text{COO}(\text{CH}_2)_{11}\text{S}]_2$  was prepared according to the literature<sup>20</sup>. Cy<sup>TM</sup>3 and Cy<sup>TM</sup>5 bisfunctional reactive dyes were purchased from GE Healthcare, Ltd.

### Preparation of SAMs of ATRP Initiators

The SAMs of ATRP initiators were formed on Au/Si and Au/Glass substrates. The Au/Si substrates were prepared by the thermal evaporation of 5 nm of titanium and 100 nm of gold onto silicon wafers, while the Au/Glass substrates were evaporated with 2-nm-thick Cr and 47-nm-thick Au films on a glass cover-slip (22 mm × 22 mm). The SAMs of ATRP initiators were prepared by immersing Au/Si and Au/Glass substrates in a 1 mM ethanolic solution of  $[\text{BrC}(\text{CH}_3)_2\text{COO}(\text{CH}_2)_{11}\text{S}]_2$  for 12 h at room temperature. After the formation of the SAMs, the substrates were thoroughly rinsed with ethanol several times and then dried in a stream of argon.

### Surface-Initiated ATRP (SI-ATRP) of OEGMA

We used 2 M OEGMA to obtain *p*OEGMA films with various thicknesses on gold substrates. To a sch-

lenk tube containing 0.70 mL of H<sub>2</sub>O, 2.78 mL of MeOH were added 2 mmol of Cu(I)Br, and 4 mmol of bpy, 20 mmol of OEGMA. The resulting dark red solution was bubbled with Ar gas for 10 min. SI-ATRP was initiated by transferring the mixture into a degassed schlenk tube that contained a Au/Si or Au/Glass substrate presenting ATRP initiators, and the mixture was then soaked for a specified time (3 to 480 min) under argon at room temperature. The polymerization was terminated by exposing the reaction to air and pouring water into the schlenk tube. The termination step caused the reaction solution to turn blue, indicating the oxidation of Cu (I) to Cu (II). All of the *p*OEGMA-coated substrates were thoroughly washed with deionized water and methanol in order to remove any physisorbed polymers, and then dried in a stream of argon.

#### **Activation of *p*OEGMA Films with *N,N'*-Disuccinimidyl Carbonate (DSC) and Subsequent Coupling of Ethylenediamine**

To activate the terminal hydroxyl groups of side chains in the *p*OEGMA films, the films were immersed in a dry DMF solution containing 0.1 M DSC and 0.1 M DMAP for 14 h at room temperature under an argon atmosphere. The resulting substrates were rinsed with DMF and CH<sub>2</sub>Cl<sub>2</sub>, and then dried in a stream of argon. The DSC-activated *p*OEGMA films were soaked in 10% ethylenediamine solution for 4 h at room temperature. After the reaction, the substrates were washed with deionized water and dried in a stream of argon. Subsequently, to deactivate the unreacted NHS carbonate ester groups, the substrates were immersed in a 50 mM sodium carbonate buffer (pH 8.5) for 20 min at room temperature. After that, the substrates were rinsed with deionized water and dried in a stream of argon.

#### **NHS-activated Cy3 Patterning by Microcontact Printing ( $\mu$ CP)**

PDMS stamps were prepared according to the literature using a Sylgard 184 silicone elastomer (Dow Corning)<sup>21</sup>. Briefly, a cleaned silicon wafer was spin-coated with a negative photoresist (SU8-50, MicroChem) and processed by photolithography to develop patterns on the surface of the wafer (a master). Subsequently, the master was silanized by (tridecafluoro-1,1,2,2,-tetrahydrooctyl)trichlorosilane under a vacuum for 2 h. To cast the PDMS stamp, the master was covered in a petri dish with PDMS oligomers. After curing for 6 h at 60°C, the PDMS stamp was peeled off from the master. Before use, the PDMS stamp was cleaned and oxidized by an oxygen plasma cleaner (Harrick PDC-002 at medium setting) for 1 min. For the pattern

generation of NHS-activated Cy3, the PDMS stamp was inked by spin-casting with NHS-activated Cy3 (0.2 mg/mL in ethanol). The inked stamp was brought into contact with the amine-terminated *p*OEGMA film for 60 s. The stamp was carefully peeled off and then rinsed with absolute ethanol and dried in a stream of argon.

#### **Spot Formation of NHS-activated Cy5 on *p*OEGMA Film**

For SPFS measurements, a solution of 0.2 mg/mL NHS-activated Cy5 (10  $\mu$ L in a 50 mM sodium carbonate buffer, pH 8.5 per one spot) was dropped on a *p*OEGMA film and was incubated for 1 h at room temperature. After the reaction, the substrates were washed with deionized water and dried in a stream of argon.

#### **Ellipsometry**

Ellipsometric measurements were performed using a Gaertner Scientific ellipsometer (model: L116s) equipped with a He-Ne laser ( $\lambda$  6,328Å) at an angle of incidence of 70°. The constants of the gold substrates were derived from ellipsometric measurements conducted at 5 or more locations on a bare gold substrate. The thickness was determined from ellipsometric measurements at 3 to 5 different spots (separated by at least 0.5 cm), using the recorded substrate constants and assuming that the refractive index of the film was 1.46 and that the film was completely transparent to the laser beam.

#### **Contact Angle Measurement**

A Phoenix 300 apparatus (Surface Electro Optics Co. Ltd., Korea) equipped with a video camera was used to measure the static contact angle on water drops of ~3  $\mu$ L in volume.

#### **Surface Plasmon Resonance (SPR) Analysis**

The thicknesses of *p*OEGMA films were measured using an SPR method. The *p*OEGMA films with various thicknesses on Au/Glass were used for analysis. The backside of the Au/Glass substrate is attached on the flat surface of a hemi-cylinder prism using an index matching oil between them so that the interface is ignored optically. A TM-polarized He-Ne laser was used to measure the reflections at each angle within a range of 35 to 75 degrees.

#### **Fluorescence Spectroscopy**

The fluorescence of the Au/Glass substrates patterned with Cy3 by microcontact printing were observed and photographed using a Nikon Eclipse ME-600 microscope (Nikon. Corp., Japan) with G-2A

filter set and digital imaging system. The Cy3 molecules covalently linked to *p*OEGMA films on Au/Si and Au/Glass substrates were exposed for 4 s.

### Fluorescence Readout

For measurements of the fluorescence intensities on the surfaces, the fluorescence images were analyzed using imaging software (GenePix Pro, ver 6.0, Axon Instruments, Inc., USA), and the mean value and standard deviation were calculated using 24 spots.

### Surface Plasmon Field-enhanced Fluorescence Spectroscopy (SPFS) Measurements

A schematic layout of the SPFS system is depicted in Scheme 1a: A TM-polarized monochromatic light (He-Ne laser,  $\lambda=632.8$  nm, Uniphase) was impinged on a hemi-cylindrical prism for SPR absorption and fluorophore excitation ( $\lambda_{\text{abs}}=649$  nm). Each Cy5-presenting *p*OEGMA film with different thickness on a Au/Glass substrate was optically coupled to a BK7 prism coupler via an index matching fluid (Cargill #5040,  $n_D=1.515$ ). Beyond the critical angle, at which total internal reflection (TIR) takes place, resonantly-absorbed plasmon-coupling was monitored using a charge-coupled device (CCD) in order to find the minimum of the reflected light. The angle of incidence was then fixed at this SPR angle, and the plasmon-enhanced fluorescence of the Cy5 dye, which is located in the locally-enhanced evanescent field, was monitored spectrally on the opposite side of the prism using a fiber-optic spectrometer (SD2000, Ocean-Optics).

### Acknowledgements

This work was supported by the Ministry of Knowledge Economy, Korea, and by Brain Korea 21 of the Ministry of Education, Science, and Technology, Korea. The ellipsometer was purchased by a research fund from the Center for Molecular Design and Synthesis.

### References

- Rich, R.L. & Myszka, D.G. Advances in surface plasmon resonance biosensor analysis. *Curr. Opin. Biotechnol.* **11**, 54-61 (2000).
- Homola, J. Present and future of surface plasmon resonance biosensors. *Anal. Bioanal. Chem.* **377**, 528-539 (2003).
- Pattanaik, P. Surface plasmon resonance: applications in understanding receptor-ligand interaction. *Appl. Biochem. Biotechnol.* **126**, 79-92 (2005).
- Liebermann, T. & Knoll, W. Surface-plasmon field-enhanced fluorescence spectroscopy. *Colloids Surf.* **171**, 115-130 (2000).
- Chu, L.-Q., Forch, R. & Knoll, W. Surface-plasmon-enhanced fluorescence spectroscopy for DNA detection using fluorescently labeled PNA as "DNA indicator". *Angew. Chem. Int. Ed.* **46**, 4944-4947 (2007).
- Yu, F., Yao, D. & Knoll, W. Surface plasmon field-enhanced fluorescence spectroscopy studies of the interaction between an antibody and its surface-coupled antigen. *Anal. Chem.* **75**, 2610-2617 (2003).
- Lakowicz, J.R. *et al.* Quenching of fluorescence. in *Principles of Fluorescence Spectroscopy*, 3<sup>rd</sup> edn. 278-330 (Springer Science+Business Media, LLC).
- Malicka, J., Gryczynski, I., Gryczynski, Z. & Lakowicz, J.R. Effects of fluorophore-to-silver distance on the emission of cyanine-dye-labeled oligonucleotides. *Anal. Biochem.* **315**, 57-66 (2003).
- Yu, F., Persson, B., Lofas, S. & Knoll, W. Attomolar sensitivity in bioassays based on surface plasmon fluorescence spectroscopy. *J. Am. Chem. Soc.* **126**, 8902-8903 (2004).
- Alcantar, N.A., Aydil, E.S. & Israelachvili, J.N. Polyethylene glycol-coated biocompatible surfaces. *J. Biomed. Mater. Res.* **51**, 343-351 (2000).
- Harris, J.M. *Poly(ethylene glycol) Chemistry: Biotechnical and Biomedical Applications* (Plenum Press, New York, 1992).
- Castner, D.G. & Ratner, B.D. Biomedical surface science: Foundations to frontiers. *Surf. Sci.* **500**, 28-60 (2002).
- Ratner, B.D. & Bryant, S.J. Biomaterials: Where we have been and where we are going. *Annu. Rev. Biomed. Eng.* **6**, 41-75 (2004).
- Lee, B.S., Chi, Y.S., Lee, K.B., Kim, Y.G. & Choi, I.S. Functionalization of poly(oligo(ethylene glycol) methacrylate) films on gold and Si/SiO<sub>2</sub> for immobilization of proteins and cells: SPR and QCM studies. *Biomacromolecules* **8**, 3922-3929 (2007).
- Sokolov, K., Chumanov, G. & Cotton, T.M. Enhancement of molecular fluorescence near the surface of colloidal metal films. *Anal. Chem.* **70**, 3898-3905 (1998).
- Malicka, J., Gryczynski, I. & Lakowicz, J.R. DNA hybridization assays using metal-enhanced fluorescence. *Biochem. Biophys. Res. Commun.* **306**, 213-218 (2003).
- Aslan, K., Lakowicz, J.R., Szmajcinski, H. & Geddes, C.D. Metal-enhanced fluorescence solution-based sensing platform. *J. Fluoresc.* **14**, 677-679 (2004).
- Cheng, D. & Xu, Q.-H. Separation distance dependent fluorescence enhancement of fluorescein isothiocyanate by silver nanoparticles. *Chem. Commun.* **3**, 248-250 (2007).
- Zhang, J. & Lakowicz, J.R. Metal-enhanced fluorescence of an organic fluorophore using gold particles. *Optics Express* **15**, 2598-2606 (2007).

20. Shah, R.R. *et al.* Using atom transfer radical polymerization to amplify monolayers of initiators patterned by microcontact printing into polymer brushes for pattern transfer. *Macromolecules* **33**, 597-605 (2000).
21. Lee, K.-B., Kim, Y. & Choi, I.S. Pattern generation of cells on a polymeric surfaces using surface functionalization and microcontact printing. *Bull. Korean Chem. Soc.* **24**, 161-162 (2003).